Electronic Supplementary Information

Quantitative understanding of thermal stability of α”-$Fe_{16}N_2$

Shinpei Yamamoto[*,1], Ruwan Gallage[1,2], Yasunobu Ogata[3], Yoshihiro Kusano[4], Naoya Kobayashi[2,5], Tomoyuki Ogawa[3], Naoaki Hayashi[1], Kaori Kohara[1,2], Migaku Takahashi[6], and Mikio Takano[1]

[1]Institute for Integrated Cell-Material Sciences (iCeMS), Kyoto University, Yoshida Ushinomiya-cho, Sakyo-ku, Kyoto 606-8501, Japan, [2]Toda Kogyo Corporation, 1-4 Meijishinkai, Otake, Hiroshima 739-0652, Japan, [3]Department of Electronic Engineering, Graduate School of Engineering, Tohoku University, 6-6-05 Aza-Aoba, Aramaki, Aoba-ku, Sendai 980-8579, Japan, [4]Department of Fine & Applied Arts, Kurashiki University of Science and the Arts, 2640 Nishinoura, Tsurajima-cho, Kurashiki-shi, Okayama 712-8505, Japan, [5]T&T Innovations Inc., 1-4 Meijishinkai, Otake, Hiroshima 739-0652, Japan, [6]New Industry Creation Hatchery Center (NICHe), Tohoku University, 6-6-10 Aza-Aoba, Aramaki, Aoba-ku, Sendai 980-8579, Japan.

Experimental procedures

XRD data were collected at room temperature (*ca*. 300 K) in transmission geometry using the Cu Kα radiation (λ= 1.54 Å) with a New D8 ADVANCE diffractometer (Bruker AXS) operated at 40 kV and 40 mA. Patterns were collected in a 2θ range from 38 ° to 90 ° with a step of 0.04 ° and an exposure time of 6 sec/step unless otherwise noted. The starting α”-$Fe_{16}N_2$ nanoparticles were sealed in borosilicate capillaries (internal diameter: 0.3 mm) under a N_2 or Ar atmosphere and then heat-treated by immersing the sealed capillaries in a preheated oil bath (473, 493, 503 and 513 K) for certain periods of time. After the heat-treatment, the glass capillaries were rapidly cooled down to room temperature and subjected to XRD measurements. Rietveld analyses were performed by using a commercially available program (TOPAS ver. 4.2). The diffractometer was calibrated by using NIST SRM640d Silicon powder as an external standard. Independently, mass spectroscopic analysis of gases evolved on heating up to 530 K (10 K/min) in flowing Ar was performed using a TG-DTA2000SA thermogravimetric/differential thermal analysis apparatus equipped with an MS9610 quadrupole mass spectrometer (Bruker AXS).

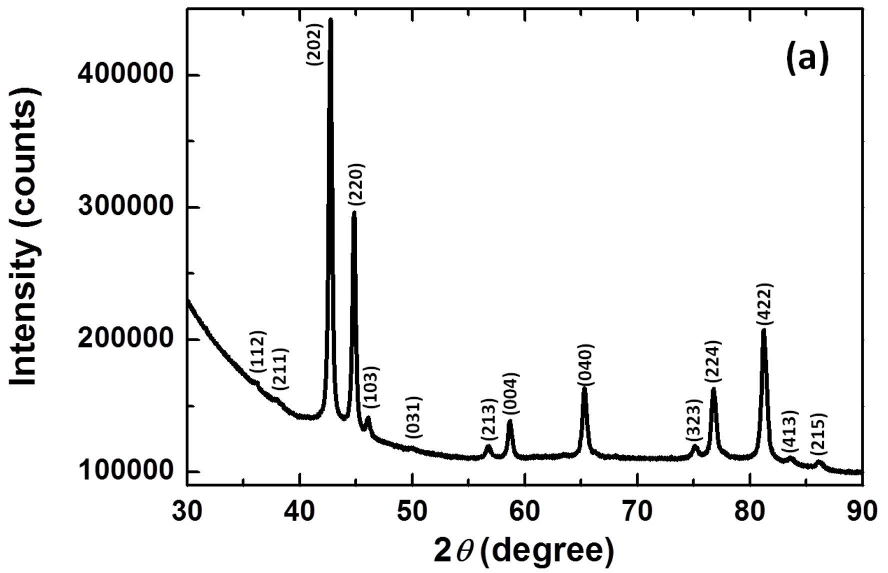

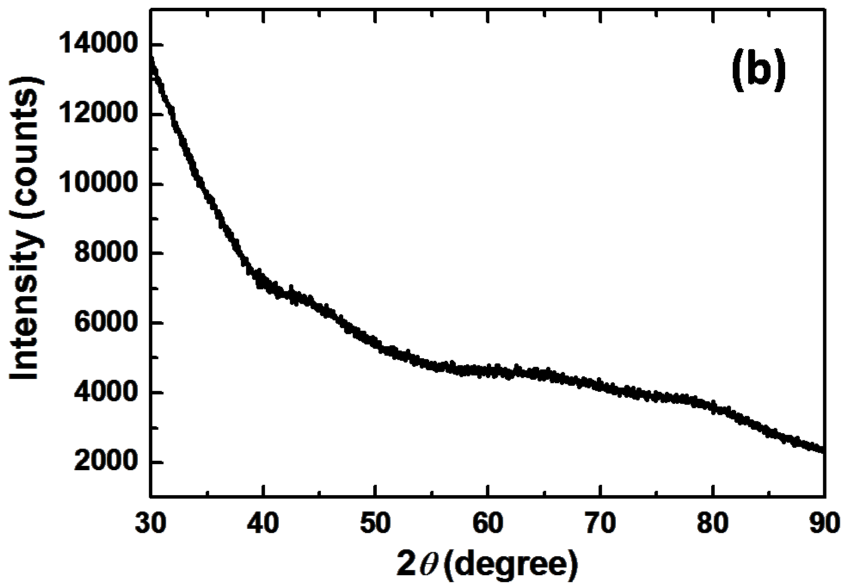

Figure S1. (a) Raw XRD pattern of the pristine α”-$Fe_{16}N_2$ nanoparticles collected in a 2θ range from 30 ° to 90 ° with a step of 0.02 ° and an exposure time of 100 sec/step. (b) Raw XRD pattern of an empty borosilicate capillary collected in a 2θ range from 30 ° to 90 ° with a step of 0.04 ° and an exposure time of 6 sec/step.

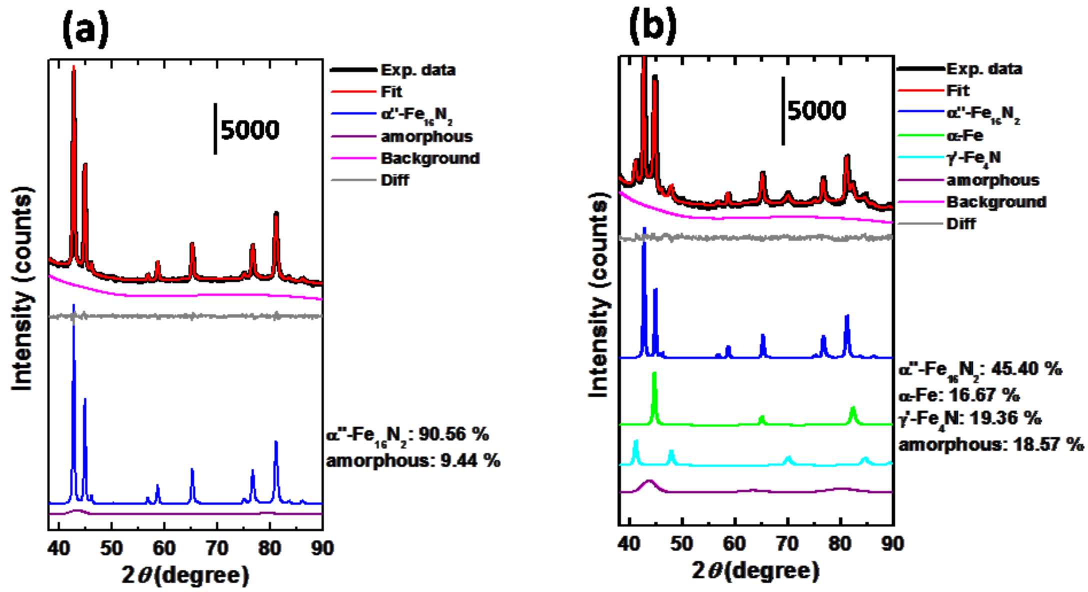

Figure S2. Typical examples of the Rietveld analyses; (a) the pristine α”-$Fe_{16}N_2$ nanoparticles and (b) the sample heat-treated for 0.2 hr at 503 K under N_2. The bars in the figures represent an X-ray intensity of 5000 counts. It should be noted here that the broad diffraction peak from glass capillary are included in the background (see Figure S1(b)).

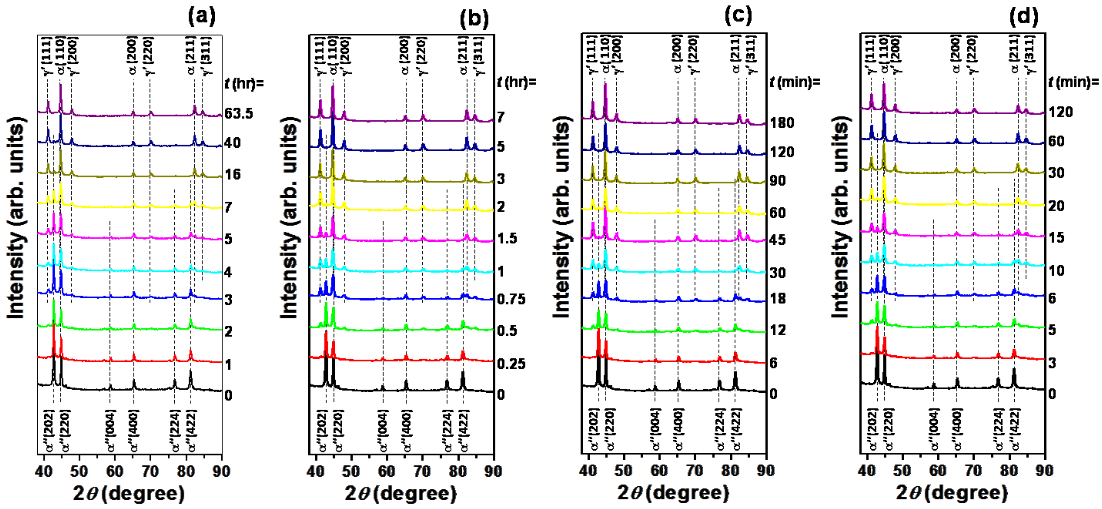

Figure S3. XRD patterns of the samples heat-treated for certain periods of time (*t*) at (a) 473 K, (b) 493 K, (c) 503 K, and (d) 513 K under N_2. Main diffraction peaks from α''-$Fe_{16}N_2$, γ'-Fe_4N and α-Fe are indicated by α'', γ' and α, respectively.

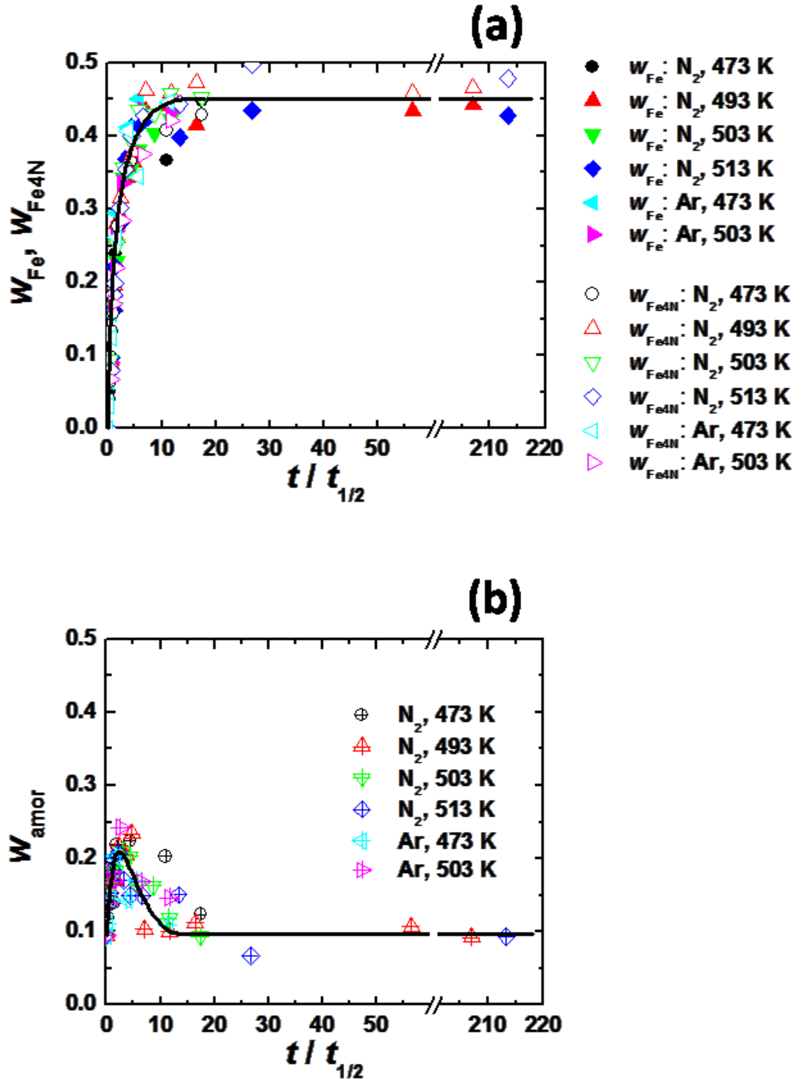

Figure S4. Plots of (a) w_{Fe} and w_{Fe4N} and (b) w_{amor} *vs*. $t/t_{1/2}$. Solid lines are guide to eyes. $t_{1/2}$ is the time when D reaches 0.5 (see Table S2 in the ESI).

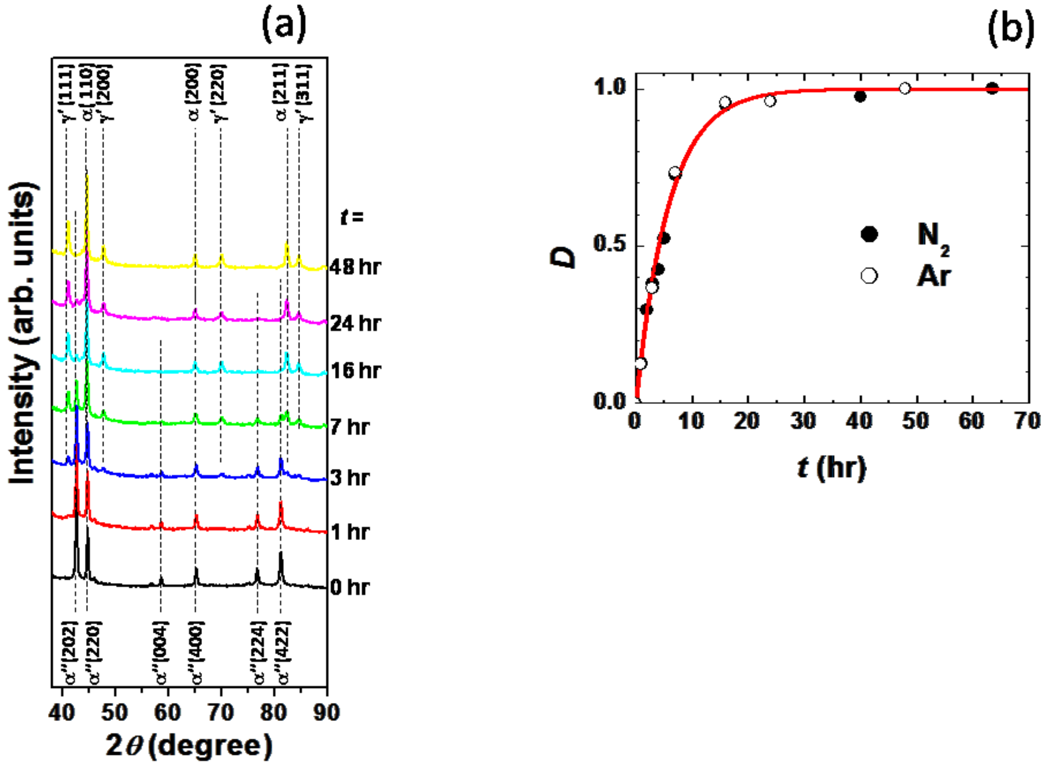

Figure S5. (a) XRD patterns of the samples heat-treated in Ar for certain periods of time (*t*) at 473 K, and (b) plot of the fraction of decomposed α”-$Fe_{16}N_2$ (*D*) as a function of heating time (*t*). Solid symbols: N_2 atmosphere, open symbols: Ar atmosphere. The solid line is the least-squares fitting using eq.(2).

Electronic Supplementary Material (ESI) for Chemical Communications

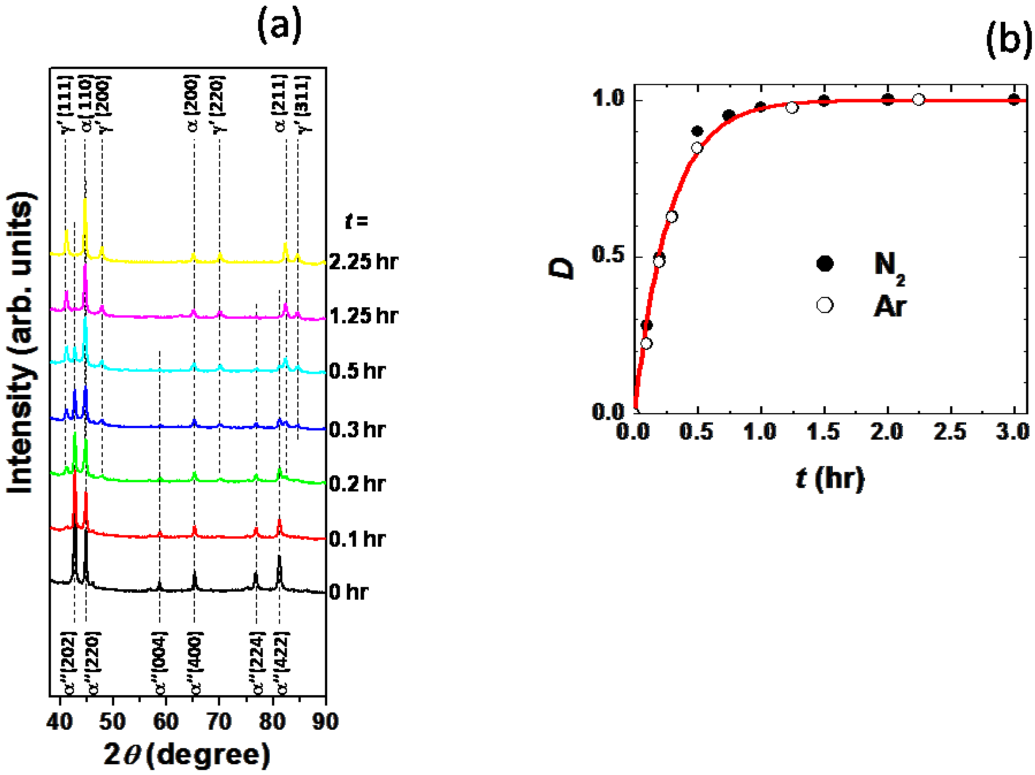

Figure S6. (a) XRD patterns of the samples heat-treated in Ar for certain periods of time (*t*) at 503 K, and (b) plot of the fraction of decomposed α"-$Fe_{16}N_2$ (*D*) as a function of heating time (*t*). Solid symbols: N_2 atmosphere, open symbols: Ar atmosphere. The solid line is the least-squares fitting using eq.(2).

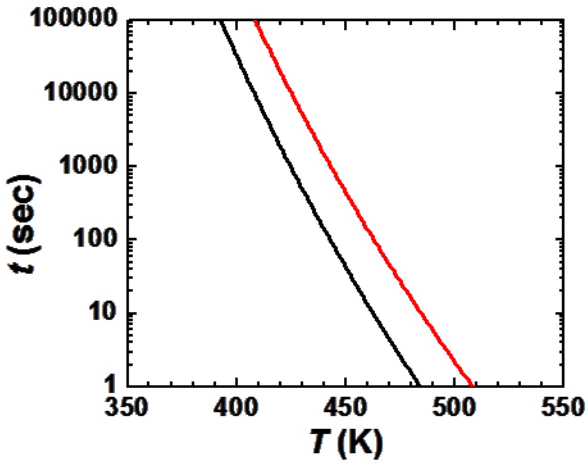

Figure S7. Thermal stability of α”-$Fe_{16}N_2$; the upper limits to which 99 % and 90 % of α”-$Fe_{16}N_2$ remain intact are shown with the black and red lines, respectively.

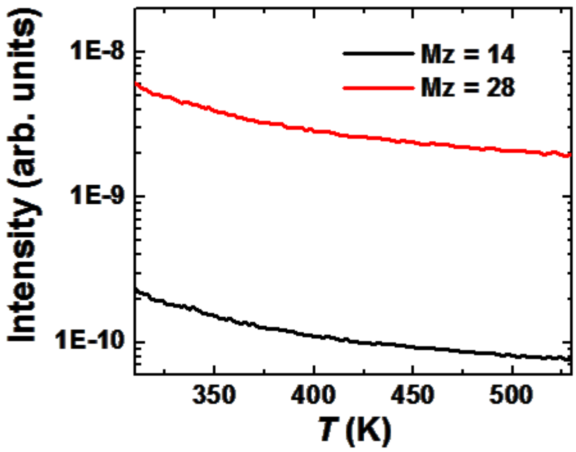

Figure S8. Mass spectroscopic data taken upon heating in Ar. Intensities for mass numbers of Mz = 14 (N) and Mz = 28 (N_2) monotonically decrease without showing any anomaly suggesting evolution of nitrogen gas during heating. The monotonic decrease indicates continuous purge of residual nitrogen by the flow.

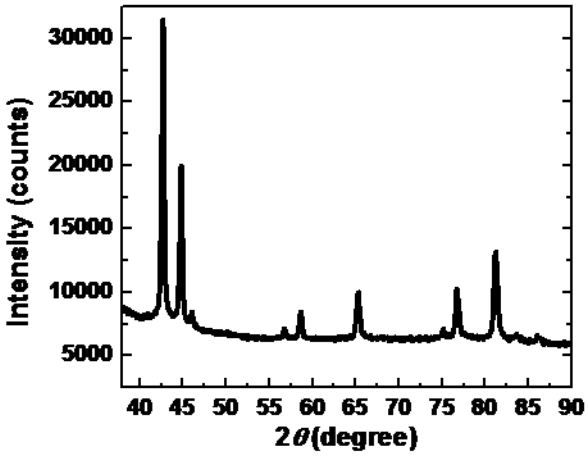

Figure S9. XRD pattern of the sample heat-treated at 373 K for 14 days under N_2. No decomposition of α”-$Fe_{16}N_2$ was observed within experimental errors.

Table S1. Rietveld refinement parameters.

Atmosphere	T [K]	t [hr]	R_{exp} [a)]	R_{wp} [b)]	S [c)]	α"-$Fe_{16}N_2$			α-Fe		γ'-Fe_4N	
						a [nm]	c [nm]	w_{Fe16N2}	a [nm]	w_{Fe}	a [nm]	w_{Fe4N}
N_2	300	-	1.15	1.31	1.14	0.5718	0.6294	0.906	--	0	--	0
N_2	473	1	1.47	1.69	1.15	0.5718	0.6291	0.791	0.2868	0.051	0.3799	0.040
N_2	473	2	1.40	1.59	1.14	0.5718	0.6292	0.638	0.2870	0.082	0.3801	0.097
N_2	473	3	1.33	1.61	1.21	0.5717	0.6291	0.562	0.2868	0.161	0.3799	0.132
N_2	473	4	1.51	1.80	1.19	0.5716	0.6291	0.522	0.2868	0.184	0.3799	0.157
N_2	473	5	1.39	1.69	1.22	0.5718	0.6292	0.431	0.2869	0.239	0.3799	0.190
N_2	473	7	1.37	1.71	1.25	0.5717	0.6293	0.250	0.2869	0.255	0.3800	0.276
N_2	473	16	1.66	2.06	1.24	0.5715	0.6299	0.051	0.2870	0.358	0.3802	0.366
N_2	473	40	1.36	1.95	1.43	0.5710	0.6308	0.023	0.2870	0.366	0.3800	0.408
N_2	473	63.5	1.38	1.85	1.34	--	--	0	0.2869	0.448	0.3801	0.429
N_2	493	0.25	1.12	1.31	1.17	0.5719	0.6293	0.666	0.2869	0.092	0.3801	0.089
N_2	493	0.5	1.11	1.47	1.32	0.5718	0.6292	0.466	0.2869	0.167	0.3800	0.195
N_2	493	0.75	1.07	1.49	1.39	0.5720	0.6295	0.289	0.2869	0.280	0.3801	0.261
N_2	493	1	1.15	1.59	1.38	0.5719	0.6296	0.176	0.2870	0.291	0.3801	0.316
N_2	493	1.5	1.15	1.59	1.38	0.5717	0.6296	0.092	0.2869	0.343	0.3801	0.359
N_2	493	2	1.54	2.14	1.37	0.5711	0.6298	0.024	0.2869	0.364	0.3800	0.377
N_2	493	3	1.15	1.74	1.51	0.5713	0.6284	0.0008	0.2869	0.433	0.3800	0.463
N_2	493	5	1.11	1.92	1.73	--	--	0	0.2869	0.442	0.3800	0.458
N_2	493	7	1.13	1.90	1.68	--	--	0	0.2869	0.415	0.3800	0.473

N_2	503	0.1	1.10	1.37	1.25	0.5718	0.62913	0.650	0.2869	0.090	0.3799	0.094
N_2	503	0.2	1.14	1.42	1.25	0.5717	0.62923	0.454	0.2869	0.167	0.3800	0.194
N_2	503	0.3	1.11	1.47	1.32	0.5718	0.6291	0.335	0.2869	0.230	0.3800	0.252
N_2	503	0.5	1.13	1.60	1.42	0.5718	0.62959	0.091	0.2870	0.343	0.3801	0.356
N_2	503	0.75	1.11	1.47	1.32	0.5714	0.62949	0.047	0.2870	0.355	0.3801	0.394
N_2	503	1	1.08	1.79	1.66	0.5714	0.63046	0.021	0.2870	0.381	0.3801	0.435
N_2	503	1.5	1.11	1.80	1.62	0.5704	0.63186	0.004	0.2869	0.404	0.3800	0.430
N_2	503	2	1.14	1.74	1.53	--	--	0	0.2869	0.423	0.3801	0.458
N_2	503	3	1.56	2.26	1.45	--	--	0	0.2869	0.454	0.3801	0.453
N_2	513	0.05	1.39	1.57	1.13	0.5717	0.6291	0.671	0.2869	0.096	0.3799	0.080
N_2	513	0.08	1.13	1.43	1.27	0.5718	0.6292	0.471	0.2869	0.161	0.3799	0.183
N_2	513	0.10	1.12	1.32	1.18	0.5718	0.6294	0.383	0.2869	0.221	0.3801	0.199
N_2	513	0.17	1.37	1.71	1.25	0.5720	0.6296	0.210	0.2870	0.281	0.3802	0.301
N_2	513	0.25	1.42	1.80	1.27	0.5717	0.6295	0.107	0.2870	0.369	0.3801	0.354
N_2	513	0.33	1.39	1.84	1.32	0.5714	0.6297	0.039	0.2869	0.412	0.3801	0.400
N_2	513	0.50	1.35	1.80	1.33	0.5711	0.6308	0.004	0.2869	0.420	0.3801	0.427
N_2	513	1.00	1.39	1.85	1.33	0.5716	0.6316	0.008	0.2869	0.398	0.3800	0.443
N_2	513	2.00	1.42	1.94	1.37	--	--	0	0.2869	0.435	0.3800	0.498
Ar	473	1	1.72	1.9	1.10	0.5718	0.6290	0.793	0.2867	0.064	0.3797	0.031
Ar	473	3	1.72	1.95	1.13	0.5717	0.6289	0.575	0.2868	0.157	0.3800	0.124
Ar	473	7	1.7	2	1.18	0.5717	0.6294	0.241	0.2870	0.295	0.3800	0.261
Ar	473	16	1.73	2.17	1.25	0.5718	0.6292	0.039	0.2869	0.411	0.3801	0.406

Ar	473	24	1.71	2.48	1.45	0.5712	0.6296	0.036	0.2870	0.451	0.3800	0.344
Ar	473	48	1.72	2.38	1.38	--	--	0	0.2869	0.444	0.3800	0.446
Ar	503	0.10	1.13	1.37	1.21	0.5718	0.6290	0.707	0.2868	0.090	0.3800	0.067
Ar	503	0.20	1.11	1.42	1.28	0.5718	0.6290	0.469	0.2869	0.184	0.3799	0.171
Ar	503	0.30	1.13	1.40	1.24	0.5719	0.6292	0.340	0.2869	0.270	0.3800	0.220
Ar	503	0.50	1.09	1.63	1.50	0.5718	0.6295	0.136	0.2870	0.332	0.3801	0.283
Ar	503	1.25	1.12	1.86	1.66	0.5715	0.6299	0.019	0.2869	0.439	0.3801	0.375
Ar	503	2.25	1.10	1.73	1.57	--	--	0	0.2869	0.432	0.3800	0.421

a) expected profile R factor

b) weighted profile R-factor

c) $S = R_{wp}/R_{exp}$

For details of the R_{exp} and R_{wp};

Young, R. A. (**1993**). "Introduction to the Rietveld method," *The Rietveld Method*, edited by R. A. Young, (Oxford University Press, Oxford), pp.1–38.

Table S2. $t_{1/2}$ values.

atmosphere	N_2				Ar	
T [K]	473	493	503	513	473	503
$t_{1/2}$ [hr]	4.31	0.48	0.19	0.09	4.21	0.19